Optics Communications 398 (2017) 91–94

Contents lists available at ScienceDirect

Optics Communications

journal homepage: www.elsevier.com/locate/optcom

Single bounce ellipsoidal glass monocapillary condenser for X-ray nano-imaging

Bowen Jiang[a,b], Zhiguo Liu[a,b], Xuepeng Sun[b], Tianxi Sun[a,b,*], Biao Deng[c,**], Fangzuo Li[a,b], Longtao Yi[a,b], Mingnian Yuan[a,b], Yu Zhu[a,b], Fengshou Zhang[a,b,*], Tiqiao Xiao[c,d], Jie Wang[c], Renzhong Tai[c]

[a] College of Nuclear Science and Technology, Beijing Normal University, Beijing 100875, China
[b] Beijing Radiation Center, Beijing 100875, China
[c] Shanghai Institute of Applied Physics, Chinese Academy of Sciences, Shanghai 201800, China
[d] University of Chinese Academy of Sciences, Beijing 100049,China

ARTICLE INFO

Keywords:
Single bounce ellipsoidal monocapillary
Monocapillary quality
Slope error
X-ray test

ABSTRACT

A single bounce ellipsoidal glass monocapillary was designed and fabricated and its performance was measured by both an optical measurement and an X-ray test. This monocapillary had a slope error of 17 μrad. The images of the focal spot and the far-field pattern recorded by a CCD detector showed that this fabricated monocapillary had high quality and satisfied the requirement of the designed data for X-ray nano-imaging.

1. Introduction

Today, X-ray nano-imaging has a wide range of applications in many fields such as energy, environment, food, medicine, biology, etc. One of the key aspects of this technology is how to focus the X-ray [1–12]. In full-field X-ray nano-imaging, the most commonly used condenser devices are zone plates and ellipsoidal monocapillaries. However, zone plates have low diffraction efficiency and limitations in bandwidth [13,14]. Moreover, their fabrication limits their aperture size. Accordingly, zone plates have a restricted range of application, especially in the high-energy range. In contrast, the transmission efficiency of ellipsoidal glass monocapillary X-ray focusing optics is higher than that of zone plates. Therefore, ellipsoidal monocapillaries are generally adopted as focusing lenses in full-field transmission X-ray nano-imaging. Consequently, much attention has been focused on the development of ellipsoidal monocapillaries [15–17]. There are two ways to fabricate such monocapillaries: the mold and drawing tower methods. A chemical treatment is necessary in the post-production of the mold procedure. This treatment may affect the roughness of the inner surface in the monocapillary and consequently influence the quality of the optics. However, the drawing-tower method does not need such a chemical pretreatment. Therefore, many researchers use the drawing tower method to fabricate ellipsoidal monocapillaries.

In X-ray nano-imaging, the requirement on the slope error of the monocapillary is very strict [18], which means that the fabrication technology of the monocapillary has to be very precise. In this paper, a new constant-temperature furnace was used to draw single-bounce ellipsoidal glass monocapillaries for use as X-ray focusing optics. We will also discuss the performance of the monocapillaries.

2. Methods

Table 1 provides the parameters of an ideal monocapillary for X-ray nano-imaging. To meet these requirements, we used silicate glass as our raw material. In the process of drawing the monocapillary, we applied a software-based procedure to control the drawing tower with a constant temperature field. This constant temperature furnace was used to heat a small-section uniform tube. Then, by changing relevant parameters, we can make the ellipsoidal monocapillary. After the fabrication of the monocapillary, we need to know whether the fabricated optics satisfies the design requirement. The slope error measured in μrad rms is one way to address this, because it represents the deviation between the ideal and real shapes. The slope error of the monocapillary would lead to a blur in the focal plane and accordingly affect its focusing quality [13]. Therefore, we could change the drawing parameters based on the slope error to improve the quality of the monocapillary. To meet these requirements, we applied an optical measurement to evaluate the diameter and straightness errors to

* Corresponding authors at: College of Nuclear Science and Technology, Beijing Normal University, Beijing 100875, China.
** Corresponding author at: Shanghai Institute of Applied Physics, Chinese Academy of Sciences, Shanghai 201800, China.
E-mail addresses: stxbeijing@163.com (T. Sun), dengbiao@sinap.ac.cn (B. Deng), fszhang@bnu.edu.cn (F. Zhang).

http://dx.doi.org/10.1016/j.optcom.2017.04.035
Received 7 October 2016; Received in revised form 12 April 2017; Accepted 16 April 2017
Available online 22 April 2017

Table 1
Designed parameters of the ellipsoidal monocapillary.

Parameter	Ellipsoidal monocapillary
Energy (keV) (Cu-target X-ray tube)	8.04
Length(mm)	32.424
Receiving aperture (mm)	0.636
Exit aperture (mm)	0.622
The distance between the center of monocapillary and the X-ray source (mm)	291.202
The distance between the center of monocapillary and focal spot (mm)	208.798
Major semi axis (mm)	250.000
Minor semi axis (mm)	0.320
Working distance (mm)	192.586
Compression ratio	0.72

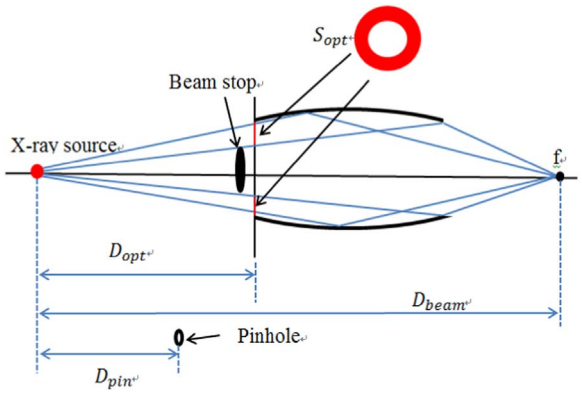

Fig. 1. The sketch of measuring the transmission efficiency and the gain in power density of monocapillary.

obtain the slope error. A digital micrometer device was used to measure the outline profile of the ellipsoidal monocapillary. According to the ratio between the outer (OD) and inner diameter (ID), the profile of inner surface could be obtained from the measured data.

The quality of the monocapillary was also tested by an X-ray source besides the optical measurement mentioned above. The X-ray test was a convincing and direct method to determine the quality of the optics. In the X-ray test experiment, we used a Cu X-ray tube whose spot size was 60 μm in diameter. An X-ray CCD camera with a 6.5-μm pixel size was used to align the optic device and obtain the image of the focal spot and far-field pattern of the monocapillary. In the test, the X-ray source was positioned 291.202 mm away from the ellipsoidal monocapillary center according to the parameters of Table 1. The monocapillary, CCD camera, and X-ray tube were each adjusted by five-dimensional stages.

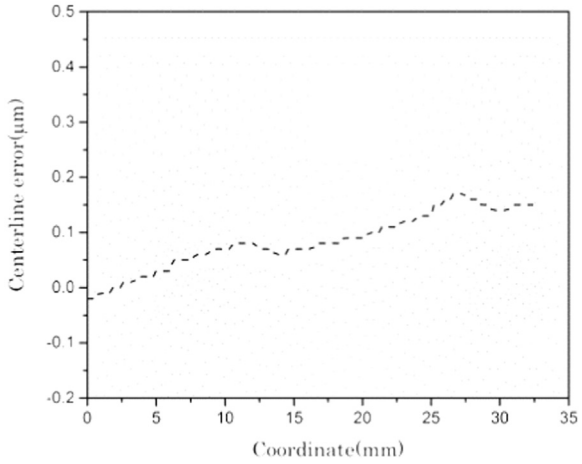

Fig. 3. The centerline straightness of the ellipsoidal monocapillary.

A beam stop in front of the monocapillary was used to block the X-rays that pass straight through the monocapillary without total reflection. The transmission efficiency of the monocapillary is defined as the ratio of the X-ray intensity transmitted through the monocapillary to the X-ray intensity at the effective entrance to the monocapillary. The transmission efficiency as a function of energy is important for all types of capillary X-ray optics. It can be measured with a pinhole and an energy dispersive detector [19]. The transmission efficiency of the monocapillary could be obtained by comparing the X-ray counts of the energy spectra from the monocapillary and a pinhole as following [19]:

$$\eta = \frac{N_{opt}}{N_{pin}} \times \frac{S_{pin}}{S_{opt}} \times \left[\frac{D_{opt}}{D_{pin}}\right]^2 \quad (1)$$

where N_{pin} is the collected counts from the pinhole at a certain energy, N_{opt} the collected counts from the optics at a certain energy, and S_{pin} the area of the pinhole entrance. S_{opt} is the area of the effective entrance to the monocapillary, which here is the area of a circular ring (Fig. 1). D_{opt} is the distance between the optics input and the X-ray source and D_{pin} is the distance between the pinhole and X-ray source.

The gain in power density of the monocapillary, which is the ratio between the power density at the focal spot with and without the monocapillary, could also be obtained by a similar measurement as following:

$$G = \frac{N_{opt}}{N_{pin}} \times \frac{S_{pin}}{S_{beam}} \times \left[\frac{D_{beam}}{D_{pin}}\right]^2 \quad (2)$$

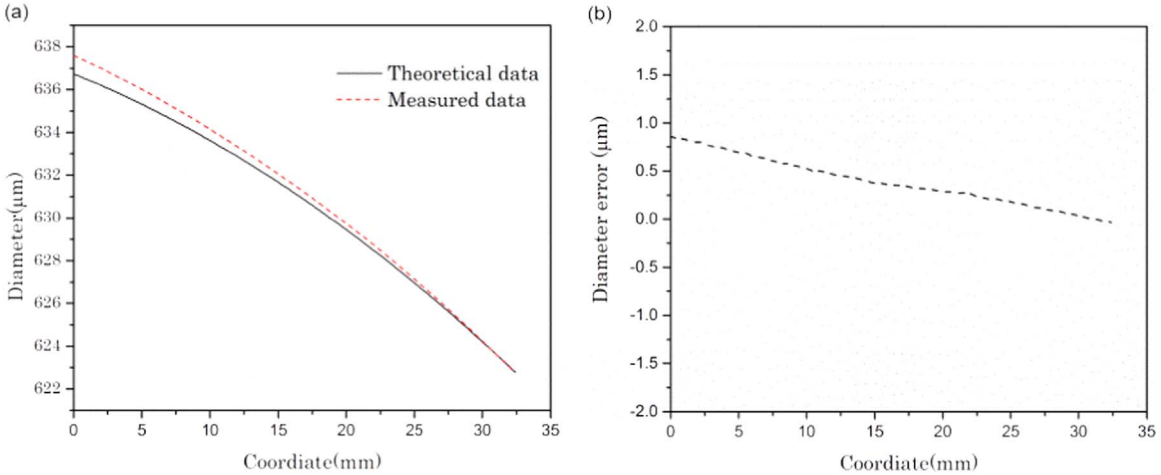

Fig. 2. (a)The optical test result of the inner diameter of the ellipsoidal monocapillary; (b) The inner diameter error.

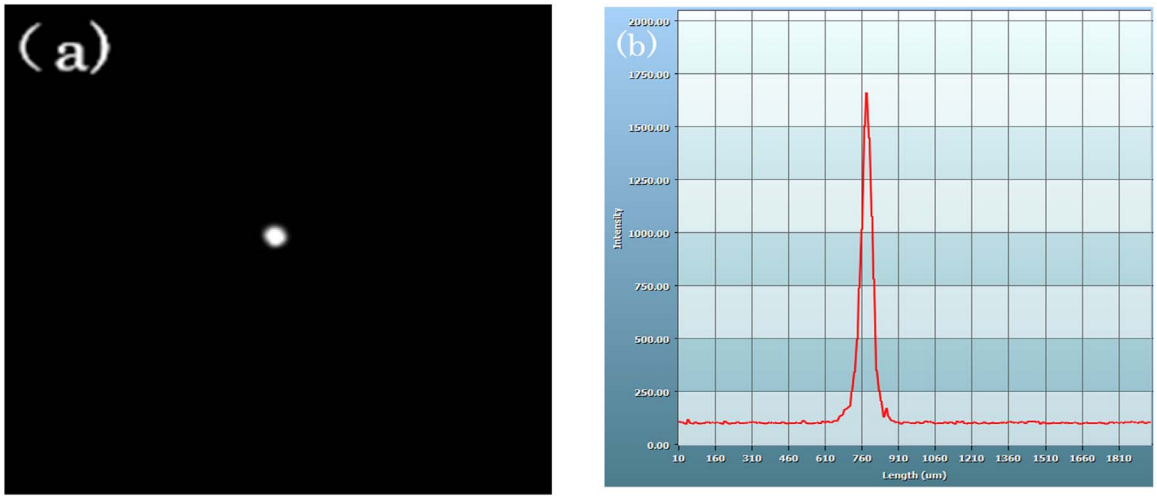

Fig. 4. (a) The image of the focal spot of the monocapillary; (b) The intensity profile of focal spot.

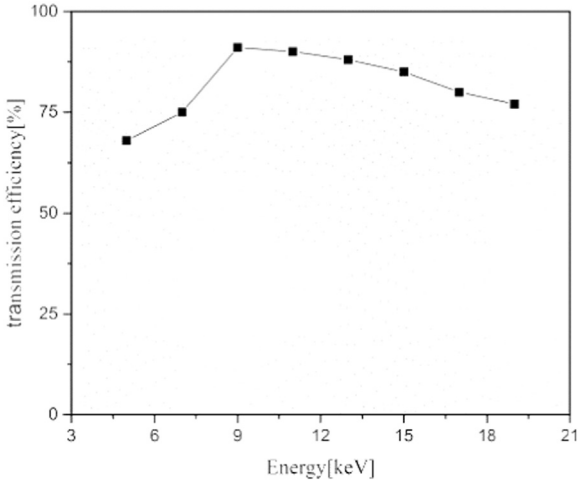

Fig. 5. Energy dependence of transmission efficiency for the monocapillary.

Here S_{beam} is the area of the focal spot of the monocapillary, S_{pin} the area of the pinhole entrance, D_{beam} the distance between the focal spot and the X-ray source, and D_{pin} the distance between the pinhole and the X-ray source.

3. Results and discussion

The quality of this optics was first established by an optical measurement. As shown in Fig. 2(a), the real profile of the inner surface of the monocapillary is close to the designed one. To provide a more detailed comparison, the diameter error between the theoretical and real shape of the monocapillary is shown in Fig. 2(b). The corresponding slope error of the diameter is 11 μrad rms. The centerline error of the monocapillary is shown in Fig. 3 and the corresponding straightness error is 13 μrad rms. According to the diameter and straightness errors, the total slope error of the monocapillary is $\sqrt{11^2 + 13^2} = 17$ μrad rms. This total slope error of the monocapillary, which is smaller than the designed value of 50.0 μrad, shows that our fabrication process meets the requirement of the X-ray nano-imaging technology.

In the X-ray test, we first measured the X-ray intensity reflected by the optics at different positions to determine the real focal spot position. The distance between the center of the monocapillary and the real focal spot was 206 mm. This value was a bit smaller than the theoretical focal spot distance, 208.798 mm. Fig. 4 shows the recorded image of the focal spot and the corresponding intensity profile of the monocapillary. The full width at the half maximum (FWHM) of the focal spot (Fig. 4(b)) is 50.0 μm. This spot size is slightly bigger than the theoretical value of 43.2 μm because the small slope error causes a blur at the focal spot. In addition to the focal spot size, the transmission

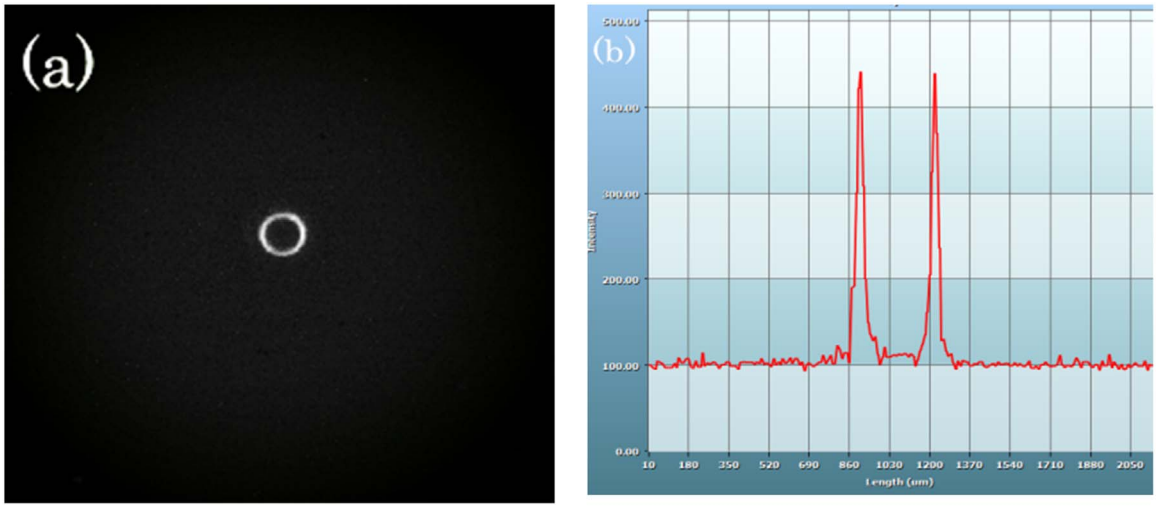

Fig. 6. (a) The far-field pattern of the monocapillary; (b) The intensity profile of the ring along the diameter.

efficiency and gain are another two important parameters to characterize the performance of optics. The energy dependence of the transmission efficiency of the monocapillary is shown in Fig. 5. As shown in Fig. 5, the transmission efficiency decreases at lower energies below about 9 keV. This can be explained by the increase of the absorption of photons with lower energies by the monocapillary wall. The decrease of transmission efficiency with the increasing energies above about 9 keV, which is shown in Fig. 5, is mainly caused by the decrease of the critical angle of total reflection with higher energies. The gain of the ellipsoidal monocapillary at the focal spot at 8.04 keV was 102, which was reached by the method mentioned above. Moreover, the far-field pattern recorded by the CCD camera at 90 mm from the focal spot of the monocapillary is shown in Fig. 6(a). This far-field pattern (Fig. 6) produced by the ellipsoidal monocapillary is helpful for evaluating the quality of the lens. As shown in Fig. 6(a), we can see that the ring is round. The intensity profile of the ring along the diameter is uniform as shown in Fig. 6(b), which satisfies the requirement of X-ray nano-imaging.

4. Conclusions

In this paper, we presented the fabrication and test of an ellipsoidal monocapillary condenser for X-ray nano-imaging. The slope error and the gain of this monocapillary were 17 μrad and 102 at 8.04 keV, respectively. These parameters meet the requirement for X-ray nano-imaging. Moreover, this optics has potential applications in other fields, such as X-ray fluorescence, X-ray diffraction, and small angle scattering.

Acknowledgements

This work was supported by the National Natural Science Foundation of China (No.11375027, No.11675019) and the Fundamental Research Funds for the Central Universities (No. 2014kJJCA03).

References

[1] David A. Shapiro, Young-Sang Yu, Tolek Tyliszczak, Jordi Cabana, Rich Celestre, Weilun Chao, Konstantin Kaznatcheev, A.L. David Kilcoyne, Filipe Maia, StefanoMarchesini, Y. Shirley Meng, Tony Warwick, Lee Lisheng Yang, Howard A. Padmore, Chemical composition mapping with nanometer resolution by soft X-ray microscopy, Nat. Photonics 8 (2014) 756–769.
[2] A. Sakdinawat, D. Attwood, Nanoscale X-ray imaging, Nat. Photonics 4 (2010) 840–848.
[3] D.X. Balaic, K.A. Nugent, Z. Barnea, R. Garrett, S.W. Wilkins, Focusing of X-rays by total external reflection from a paraboloidally tapered glass capillary, J. Synchrotron Radiat. 2 (1995) 296–299.
[4] S.A. Hoffman, D.J. Thiel, D.H. Bilderback, Developments in tapered monocapillary and polycapillary glass X-ray concentrators, Nucl. Instrum. Methods A 347 (1–3) (1994) 384–389.
[5] R. Huang, D.H. Bilderback, Simulation of microfocused image size from a one-bounce glass capillary, Nucl. Instrum. Methods A 467 (2001) 978–981.
[6] T. Sun, X. Ding, Confocal X-ray technology based on capillary X-ray optics, Rev. Anal. Chem. 34 (1–2) (2015) 45–59.
[7] A. Snigirev, V. Kohn, I. Snigireva, B. Lengeler, A compound refractive lens for focusing high-energy X-rays, Nature 384 (6604) (1996) 49–51.
[8] S. Suehiro, H. Miyaji, H. Hayashi, Refractive lens for X-ray focus, Nature 352 (6334) (1991) 385–386.
[9] W.B. Yun, P.J. Viccaro, B. Lai, J. Chrzas, Coherent hard X-ray focusing optics and applications, Rev. Sci. Instrum. 63 (1) (1992) 582–585.
[10] C.G. Schroer, Focusing hard X rays to nanometer dimensions using Fresnel zone plates, Phys. Rev. B 74 (3) (2006).
[11] K. Saitoh, K. Inagawa, K. Kohra, C. Hayashi, A. Iida, N. Kato, Fabrication and characterization of multilayer zone plate for hard X-rays, Jpn. J. Appl. Phys. Part 2-Lett. 27 (11) (1988) L2131–L2133.
[12] B. Lai, W.B. Yun, D. Legnini, Y. Xiao, J. Chrzas, P.J. Viccaro, V. White, S. Bajikar, D. Denton, F. Cerrina, E. Difabrizio, M. Gentili, L. Grella, M. Baciocchi, Hard X-ray phase zone plate fabricated by lithographic techniques, Appl. Phys. Lett. 61 (16) (1992) 1877–1879.
[13] W. Yun, B. Lai, A.A. Krasnoperova, et al., Development of zone plates with a blazed profile for hard X-ray applications, Rev. Sci. Instrum. 70 (9) (1999) 3537–3541.
[14] A.V. Baez, Fresnel zone plate for optical image formation using extreme ultraviolet and soft X radiation, JOSA 51 (4) (1961) 405–412.
[15] X. Zeng, F. Duewer, M. Feser, C. Huang, A. Lyon, A. Tkachuk, W. Yun, Ellipsoidal and parabolic glass capillaries as condensers for X-ray microscopes, Appl. Opt. 47 (13) (2008) 2376–2381.
[16] G. Hirsch, Metal capillary optics: novel fabrication methods and characterization, X-Ray Spectrom. 32 (2003) 229–238.
[17] R. Huang, D.H. Bilderback, Single-bounce monocapillaries for focusing synchrotron radiation: modeling, measurements and theoretical limits, J. Synchrotron Radiat. 13 (1) (2006) 74–84.
[18] X.P. Sun, Z.G. Liu, L.T. Yi, et al., Adjustable hollow-cone output X-ray beam from an ellipsoidal monocapillary with a pinhole and a beam stop, Appl. Opt. 54 (35) (2015) 10326–10332.
[19] T. Sun, X. Ding, Measurements of energy dependence of properties of polycapillary X-ray lens by using organic glass as a scatterer, J. Appl. Phys. 97 (12) (2005) 124904.